A REVIEW FOR FORECASTERS ON THE APPLICATION OF HODOGRAPHS TO FORECASTING SEVERE THUNDERSTORMS

Charles A. Doswell III

National Severe Storms Laboratory
Norman, Oklahoma

Abstract

Basics of the hodograph are reviewed in order to acquaint (or re-acquaint) forecasters with this useful tool for diagnosis of vertical wind shear. This review makes use of existing operational programs for hodograph analysis, as well as presenting the principles underlying their use. A brief summary is given of the physical processes acting to create vertical wind shear. These processes provide the basis for interpretation of the hodograph and an understanding of them allows one to make subjective hodograph prognoses. Finally, an explanation for the concepts of streamwise vorticity and helicity is given, emphasizing the importance of viewing them in a storm-relative framework. A representative set of references is provided, as well, to guide the forecaster in developing enough understanding of hodographs to apply them to severe thunderstorm forecasting.

1. Introduction

With the development of automated procedures for plotting and analysis of upper-air data, many forecasters may have forgotten (or never learned) the diagnostic skills necessary for interpreting the information contained in the vertical wind profile. This is especially unfortunate because recent research has shown that the character of the wind profile can have a strong control on thunderstorm behavior in a given thermodynamic environment. Although the research is not yet complete, the results so far indicate that the revival of the hodograph as a thunderstorm forecasting tool is quite worthwhile, especially in recognizing the potential for supercell thunderstorms, which can be devastatingly destructive, even when non-tornadic.

The threat of supercells is quite variable across the nation. For those in regions where supercells (tornadic or not) are rare, it is possible to conclude that it is a waste of time to study the tools of the severe thunderstorm forecasting trade. I contend that this is an erroneous conclusion. The threat of a supercell-related disaster looms quite large in those regions precisely because such storms are relatively rare but not impossible (see, e.g., Braun and Monteverdi 1991). When a supercell (especially one with a tornado) occurs in an area of low supercell frequency, forecasters may not recognize the seriousness of the impending event, at least in part because they are not accustomed to dealing with such events and may not be familiar with (or using) the relevant forecasting tools (see discussions by Gonski et al. 1989, and Korotky 1990).

These notes are intended to acquaint (or re-acquaint) forecasters with the hodograph, an especially useful tool for revealing the key features in the wind profile. While the primary emphasis will be recognition of supercell potential, I am including some discussion of the hodograph's value in other forecasting and analysis issues. I cannot overemphasize the importance of pursuing the topics I have reviewed via the references, since this review is necessarily incomplete.

2. Basics of the Hodograph

A vertical wind profile consists of a set of wind speeds and directions at various heights. Forecasters are probably most familiar with the sort of vertical wind plot shown in Figure 1, produced by the plotting programs in the Automation of Field Operations and Services (AFOS) system. The data used in this plot are shown in Table 1.

Operational forecasters should recognize that wind data as provided by operational soundings include wind speed and direction at each mandatory pressure level and at a set of pre-specified heights. The plot shown in Figure 1 is especially effective at showing the veering and backing of the wind with height, but it is difficult to use this plot to visualize the effect of changing wind speeds with height. In the next section, I will discuss some of the processes which influence the change of wind (speed and direction, both) with height, but for now I want to concentrate on the hodograph.

The AFOS applications program developed by Stone (1988) called CONVECT allows the forecaster to get a hodograph plotted. Using the same data shown in Figure 1 and Table 1, the resulting plot is shown in Figure 2. What does this plot really represent? It is well-known that specification of a vector requires two quantities; for wind vectors, this often takes the form of speed and direction. When the wind vector is given in this way, it implies a *polar* representation of the wind: the direction determines an angle and the speed gives the length of the vector along that angle. Figure 3 shows such a polar representation. Everyone should recognize this sort of plotting diagram; radar is done similarly.

It also is well-known that there is at least one other way to represent a vector. That is, one specifies an *orthogonal Cartesian* representation of the wind by giving special significance to two mutually perpendicular wind directions. These are the Cartesian coordinates in this representation of the vector; by convention, these coordinates are usually taken to be east-west (the so-called u-component) and north–south (the so-called v-component). The (horizontal) wind vector is specified completely by giving the u and v components of the wind. Thus, the horizontal vector wind V_H is described as the sum $u\mathbf{i}+v\mathbf{j}$, where **i** and **j** are unit vectors in the east–west and north–south directions: **i** generally is taken to point eastward and **j** northward, so positive u is a westerly wind and positive v is a southerly wind.

At this point, it is important to remember that these are vector representation systems, distinct from what we ordinarily think of as coordinate systems. To see this, consider where the vertical wind profile was taken; its *location* can be given by latitude and longitude, or by saying it is so many miles in some direction from point with a known position, or by giving its position as some number of kilometers east and another number of kilometers north of some known point. All these are different ways of representing the location of the wind profile as a vector from some origin, and location is what one usually thinks of when talking about coordinate

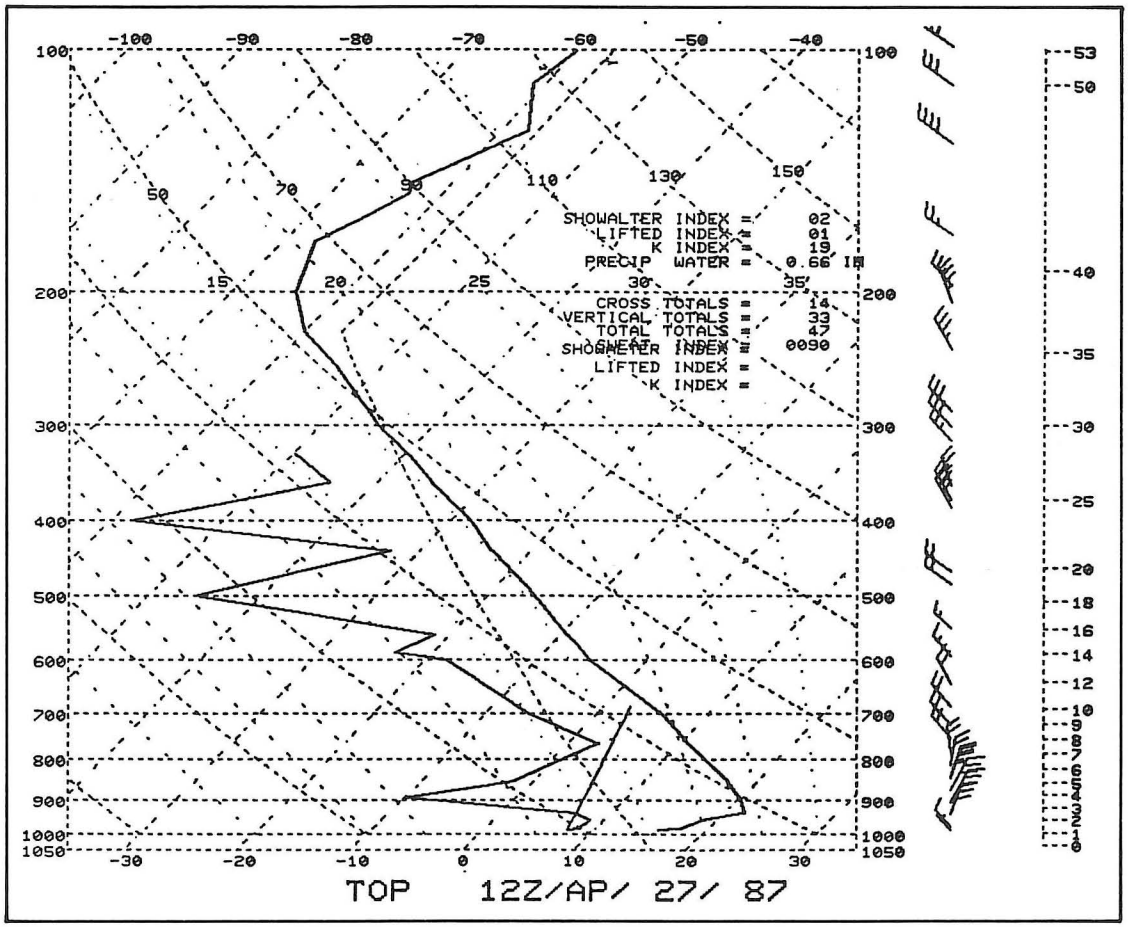

Fig. 1. Conventional AFOS skew-T, log p plot of data from Table 1.

Table 1. Mandatory and significant level data for Topeka, Kansas, 1200 UTC 27 April 1987.

```
TOPMANTOP
WOUS00 KTOP 271200
72456 TTAA  77121 72456 99988 15658 32005 00158 ///// /////
85557 17269 02027 70179 05662 32520 50582 15980 31022 40746
28380 33028 30945 451// 32530 25064 543// 33033 20204 645//
32026 15379 631// 30035 10631 601// 30529 88172 673// 30527
77999 51515 10164 00003 10194 01527 34521=
TOPSGLTOP
WOUS00 KTOP 271200
72456 TTBB  7712/ 72456 00988 15658 11984 17459 22958 18660
33938 21665 44894 19880 55764 10658 66601 05363 77589 06567
88560 09562 99500 15980 11438 23759 22400 28380 33356 35359
44327 39960 55226 601// 66172 673// 77145 637// 88126 577//
99110 613// 11100 601//=

PPBB  77120 72456 90012 32005 32508 02028 90345 03034 03032
02026 90678 01022 35019 32520 909// 32022 91246 33021 32016
31514 92056 31022 33029 33527 929// 32527 93058 32529 33033
33537 939// 32523 9427/ 30525 30542 9502/ 31032 30530=
```

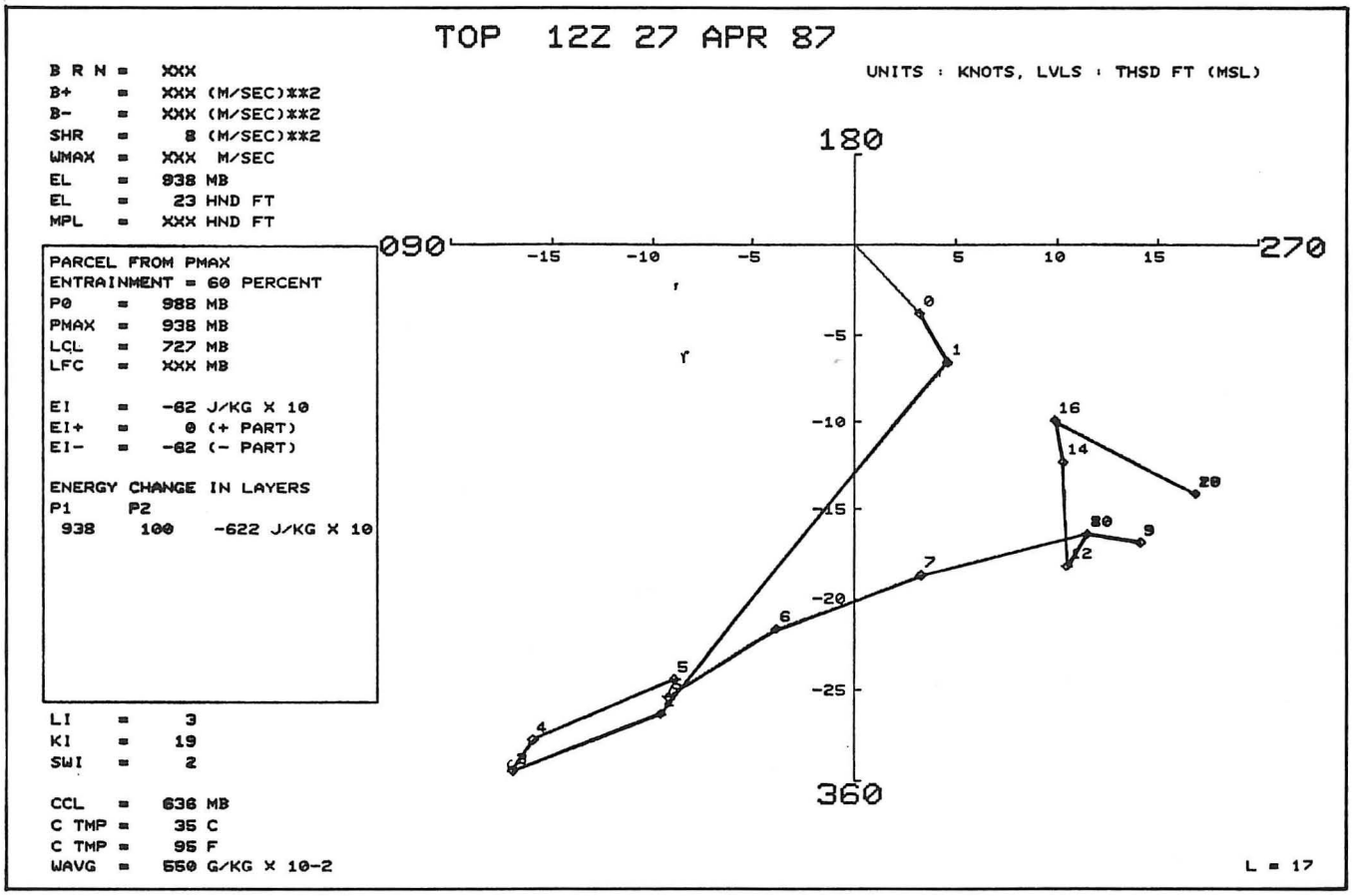

Fig. 2. Output from the CONVECT applications program in AFOS for the data from Table 1.

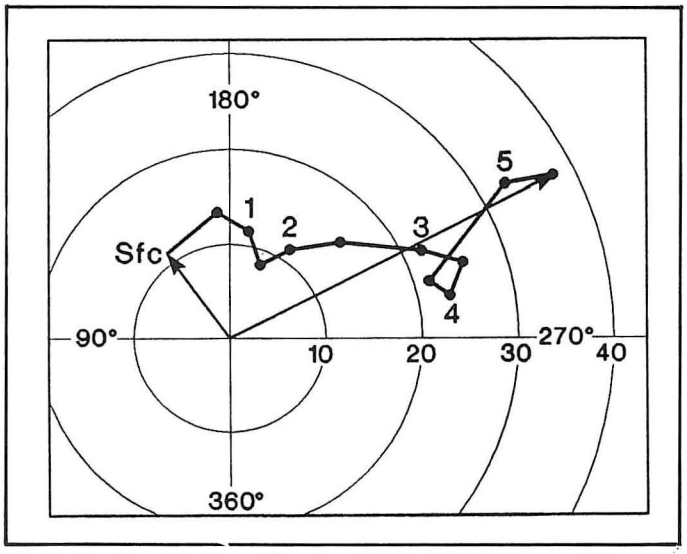

Fig. 3. Hodograph plotted in polar representation form, using speed and (meteorological) wind direction. Circles are wind speed every 10 m s^{-1}, hodograph heights (AGL) labelled in km, every 0.5 km. Data are hypothetical.

systems. In the case of the hodograph, the origin is taken to be a calm wind (although one may choose to move the origin—see section 6), and the wind at a particular level is given by a vector from the origin to that point on the graph corresponding to that particular wind.

Now the vector connecting two points is not changed when the coordinate system is changed, but the *components* of the vector representation do, indeed, change when changing coordinates. Thus, no matter how the wind vectors are represented, the points corresponding to the wind vectors themselves do not change. It certainly would be disturbing if we could change the winds simply by changing the way we represent them on a diagram!

The CONVECT program uses u and v components to display the wind vectors,[1] but the plot would look identical if the program used speed and direction. However, if the winds were shown in a *moving* coordinate system (e.g., one moving with constant speed), the vectors indeed would change; additional discussion of this issue is deferred to section 6.

When plotting the wind vectors, if the tails of the vectors are all put at the origin, one needs to label the tips of the vectors with the heights at which each wind vector applies, to distinguish them from each other. Since the winds generally change with height, the vector tips should trace out some line in going from level to level.

[1]Note that the CONVECT program scales the hodograph plots so that the result is more or less the same size, regardless of the magnitude of the shears. This can be deceiving, as a hodograph with little or no shear may be scaled to look like a hodograph with large shear. Thus, users of this program are cautioned to examine the plots carefully. It would be better to have the coordinates remain the same for all plots, making the difference between a low-shear case and a high-shear case more apparent visually.

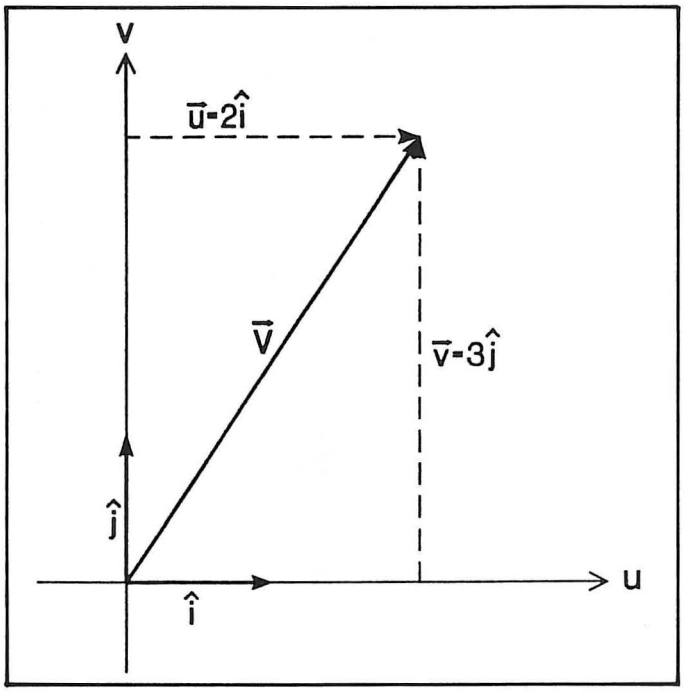

Fig. 4. Schematic showing the wind component representation, with **i**- and **j**-unit vectors. In this example, the u-component is 2 units and the v-component is 3 units.

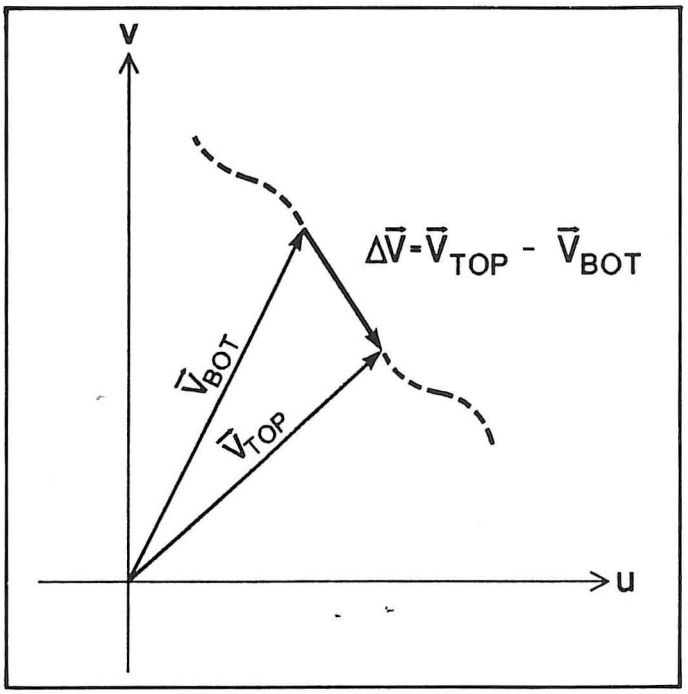

Fig. 5. Two levels in a wind hodograph (dashed), showing the shear vector, $\Delta\mathbf{V}$, as the difference between the top and the bottom levels.

In looking at the plot in Figure 2, the line connecting the tips of the plotted wind vectors is the *hodograph*. Thus, the hodograph shows how the wind changes with height, which is the *vertical wind shear*. The wind shear is also a vector, defined as the vector difference between winds at different levels.[2] For any two points along the plot, the wind shear vector between those levels makes up a segment of the hodograph (Fig. 5). When the wind direction turns counterclockwise with height, one says that the wind is *backing* and when it turns clockwise, the wind is said to be *veering*. This much one can see readily from a plot such as Figure 1.

However, this takes no account of the wind *speed* information; the speed has nothing to do with whether or not the wind is backing or veering with height. The wind certainly can change speed with height even when the direction remains constant. The difference between two levels gives the shear vector, but we need at least *three* levels to see the *change* of the shear vector with height. Clearly, a proper representation of this requires both speed and direction information. This is illustrated in Figure 6; when the shear vector backs with height, the hodograph is turning counterclockwise and when the shear vector veers with height, the hodograph is turning clockwise.

Finally, when looking at Figure 2, it is apparent that real data can have much more "structure" in the vertical than is shown in the schematic hodographs seen in many research papers. To some often unknown extent, a part of that structure is simply observation noise. Further, when there is very little shear over several layers, the vectors get crowded together and may do some loop-de-loops in a small space.

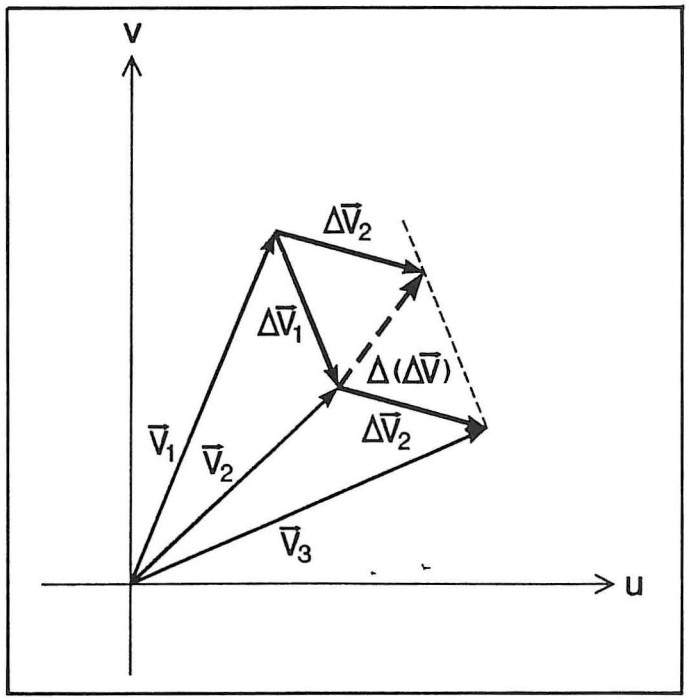

Fig. 6. Three levels in a wind profile, showing the two shear vectors, $\Delta\mathbf{V}_1$ and $\Delta\mathbf{V}_2$, and the change of the shear vector in the layer, $\Delta(\Delta\mathbf{V})$. Note that $\Delta\mathbf{V}_2$ has been displaced from its original position so that its tail is at the same point as $\Delta\mathbf{V}_1$, for purposes of calculating $\Delta(\Delta\mathbf{V})$.

Given the fact that real wind data include errors as well as valid observations of what is going on, one should look at the broad features of the hodograph and not try to make too much of the details.

[2]On Figure 2, the CONVECT program has drawn a line from the origin to the surface (labelled "0") which, strictly speaking, is not part of the plot.

3. Processes Which Create Vertical Wind Shear

a. The Thermal Wind

Perhaps the most well-known contributor to vertical wind shear is the thermal wind. The basic definition of the thermal wind (V_T) is the *vertical shear of the geostrophic wind* (V_g):

$$\mathbf{V}_T = -\frac{\partial \mathbf{V}_g}{\partial p} = -\frac{\partial}{\partial p}\left[\frac{\mathbf{k}}{f} \times \nabla_p \phi\right] = \frac{R}{fp}\mathbf{k} \times \nabla_p T, \quad (1)$$

where ϕ is the geopotential height, R is the gas constant for dry air, T is the temperature on a pressure (p) surface, **k** is the unit vector in the vertical, and f is the Coriolis parameter ($f = 2\,\Omega \sin \phi$; Ω is the angular velocity of the earth and ϕ is the latitude). Note that this definition of "vertical" uses pressure as the vertical coordinate. The formula shows why it is called the "thermal" wind: it is related to the temperature gradient in a way similar to the relation of the geostrophic wind to the height gradient. Just as the geostrophic wind is parallel to the height contours, with low heights to the left[3] of the geostrophic wind, and with speed inversely proportional to the spacing of the contours, so the thermal wind is parallel to the isotherms, with low temperatures to the left of the thermal wind, and with speed inversely proportional to the spacing of the isotherms.

As anyone who ever has looked at a weather map already knows, there is a pronounced tendency for the observed wind to look more or less like the geostrophic wind, especially as one goes up high enough to be out of the effects of the planetary boundary layer (which is roughly within the lowest kilometer or so above the surface). That is, the observed winds in the free atmosphere blow approximately parallel to the height contours, with low heights on the left, and with a speed more or less inversely proportional to the spacing of those contours. To the extent that the real wind is similar to the geostrophic wind, then, the vertical shear of the real wind ought to be similar to the thermal wind.

For the thermal wind to be non-zero, the geostrophic wind must change with height, by definition (1). This means that the direction and/or magnitude of the geopotential height gradient must change as one goes up. An atmosphere in which that height gradient doesn't change in the vertical is said to be *barotropic*. In such an atmosphere, there are no isotherms on a constant pressure surface, as the reader may wish to confirm. If the height gradient's direction remains the same but the magnitude changes as one goes up, the atmosphere is said to be *equivalent barotropic*.[4] The notion of equivalent barotropy comes from the observed tendency for the isotherms on constant pressure level charts to line up with the height contours—it is left for the reader to confirm that in such a case, the geopotential height gradient changes magnitude, but not direction. In such a case, the hodograph clearly is a straight line parallel to the wind. When the geopotential height gradient changes both direction and magnitude with height, the atmosphere is fully *baroclinic*. Generally speaking, the real atmosphere is always baroclinic but it may be very nearly barotropic (or equivalent barotropic) in some situations.

All this means that if the real wind and the geostrophic wind are similar, any observed wind shear in the vertical implies baroclinic conditions. The stronger the wind shear, the more strongly baroclinic the situation is—in fact, in some theoretical work, vertical wind shear is taken as synonymous with baroclinity.

Now a well-known relationship exists between the vertical change of geostrophic wind direction and thermal advection; see Doswell (1982) or Hess (1959, pp. 189 ff.) for a discussion of this topic. Summarizing the results, backing winds with height are indicative of cold advection, while veering winds imply warm advection.

b. Wind Shear in the Planetary Boundary Layer

Given the fact that the real winds look most like the geostrophic winds only above the planetary boundary layer, what happens to the wind *within* the planetary boundary layer? This subject can get quite technical in a hurry, but the essence can be understood rather simply. Assuming that the wind within the boundary layer is the result of a balance among three forces, instead of two (as in the geostrophic wind), we arrive at what has been called the *antitriptic* wind. Besides Coriolis and pressure gradient forces, one must consider a force due to friction.

The topic of antitriptic surface flow is discussed at some length in Schaefer and Doswell (1980), but the notion of importance here is that the frictional effect dies out with height, becoming negligible at the top of the so-called *planetary boundary layer* (see Fig. 7). By appropriate assumptions and algebraic manipulation, one can derive an expression for the wind through the depth of the planetary boundary layer. This expression results in a plot of the wind profile with height (a hodograph!) called the *Ekman Spiral*. The details

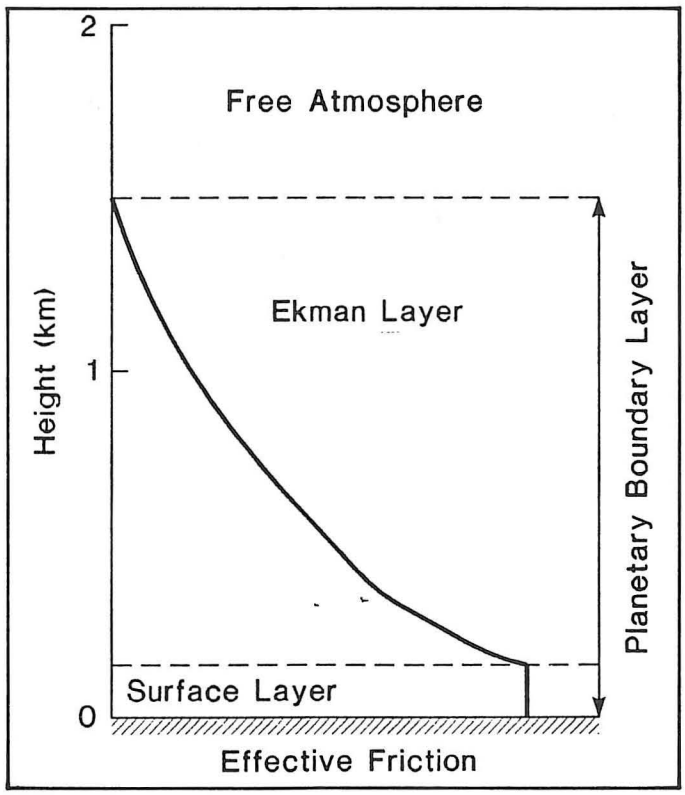

Fig. 7. Schematic showing roughly the amount of frictional effect as a function of height above the surface. The various layers referred to in the text and the references are labelled.

[3]This is true for the northern hemisphere, of course. In the southern hemisphere, one should substitute "right" for "left" and everything else remains the same.

[4]Strictly speaking, of course, such an atmosphere is baroclinic (non-barotropic), but it is a special case, clearly.

can be found in various places (e.g., see Hess 1959, Holton 1979, etc.), but the important things to see are that (a) the wind veers with height, and (b) the wind becomes indistinguishable from the geostrophic wind at the top of the planetary boundary layer.

The real wind profile that one sees can be affected by such things as baroclinity, of course, but if the Ekman Spiral has any meaning whatsoever in the real world, most soundings (in the northern hemisphere) should show veering with height in the lowest kilometer or so. The veering exhibited by an Ekman-like flow is not associated with baroclinic processes at all, and so that veering which can be accounted for by Ekman theory cannot be taken to imply warm advection. If one has a sounding that shows veering off the surface, how much of the observed veering is the result of frictional effects rather than warm advection? No simple answer exists, because atmospheric frictional effects are not well understood. Presumably, if one doesn't have warm thermal advection evident in the lower troposphere, then any observed veering in the lowest layers of the atmosphere is most likely the result of friction-related processes. An observed wind profile that backs with height off the surface means that some process is overwhelming frictional effects, probably strong cold advection.

c. Other Ageostrophic Processes

Clearly, there are other processes besides friction which result in the real wind not being well-approximated by the geostrophic wind. The situations where this can occur are generally associated with important weather systems: jet streaks aloft, rapidly moving and/or intensifying cyclones, and so on. In fact, one might argue that the geostrophic wind is closest to the real wind only when it matters the least. There is merit to this argument, but the geostrophic approximation can be remarkably effective at explaining observed events, at least qualitatively.

Any process resulting in a significant departure from geostrophic balance is going to alter the shear profile away from that predicted from the thermal wind relationship. It might be of some value, someday, to plot the thermal wind profile inferred from the temperature fields side-by-side with the observed wind shear profile. Significant departures from the inferred profile would be a signpost that something important might, indeed, be going on. As one can find from any textbook, the ageostrophic flow is directly related to accelerations in the wind field—the geostrophic wind is, by definition, not accelerated.

4. Interpreting and Forecasting the Hodograph in Convective Events

In a sense, the previous section has begun to lay the groundwork for interpreting the hodograph. Some readers might enjoy the early work on "single-station analysis" that employed some of the concepts I've described above (e.g. Oliver and Oliver 1945). The material which concludes the previous section is central to the discussion of how one infers things about the large-scale environment from a single vertical wind profile. Someone might wish to consider doing some studies of how well these ideas work in practice and how best to incorporate them into one's forecasting practice. It is not my intent to provide a "cookbook" for that purpose in this paper.

Turning to the main application considered in this paper, much of what is known about the relationship between the hodograph and thunderstorms can be stated pretty simply. The most important type of severe thunderstorm is the *supercell,* which is responsible for a disproportionate amount of damage and casualties relative to its frequency. That is, while supercells form a rather small fraction of the total number of severe thunderstorm events, they tend to be responsible for a rather large fraction of the damage and casualties associated with severe thunderstorms. This is not the place for a full discussion of the topic of supercells and/or severe thunderstorms (see Klemp 1987, Doswell et al. 1990). However, it has become apparent that supercells are associated with particular environmental shear regimes and the hodograph is the diagnostic tool of choice for this purpose. In order to forestall the inevitable question, I want to emphasize that there is no "magic" number which characterizes the necessary shear value! One can see from reading the references that shear values on the order of 10^{-3} s^{-1} and larger (roughly, 6 kt per 10 000 ft) are characteristic of severe storm environments, but this is by no means a "threshold" value.

As the amount of shear in the environment increases, with a given amount of available convective buoyant energy (i.e., instability), there is a range of shear values within which long-lived convective storms are likely (Rasmussen and Wilhelmson 1983). This range of shear values appears to depend on the amount of instability, with long-lived storms occurring in greater shears generally (but not always!) associated with larger instability. This apparent dependence on instability has not been explored conclusively, but one possible interpretation is that the likelihood of persistent storms increases with increasing instability, with a given amount of shear; conversely, it also appears that increasing shear with a given amount of instability leads to longer lifetimes for convective storms, at least up to a point.

When the hodograph is more or less a straight line (e.g., Fig. 8), the most likely development within this moderate to large range of shears is splitting storms that form more or less mirror images of one another, with one rotating cyclonically and moving to the right of the shear vector, while the other rotates anticyclonically and moves to the left of the shear vector. In an environment with a straight hodograph, neither of the pair is favored, so both storms tend to persist (e.g., Fig. 9).

As noted above, enhanced vertical shear can increase the persistence of convection, at least up to a point, and then as the shear increases beyond that, the persistence (or even development) of convection is reduced. Thus, shear appears to be beneficial to convection up to some value, beyond

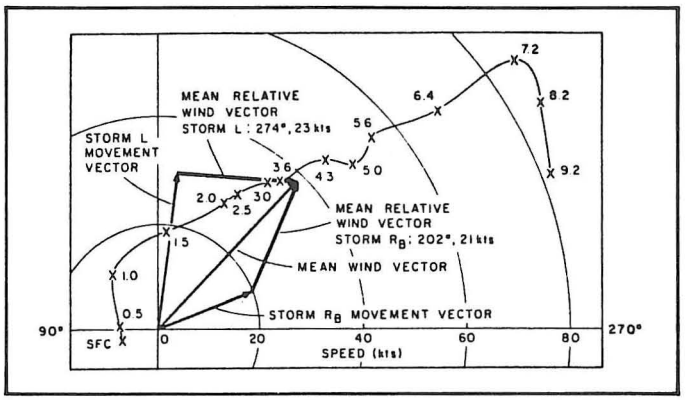

Fig. 8. Hodograph associated with storms of 3 April 1964 (from Charba and Sasaki 1971), showing a nearly straight-line character.

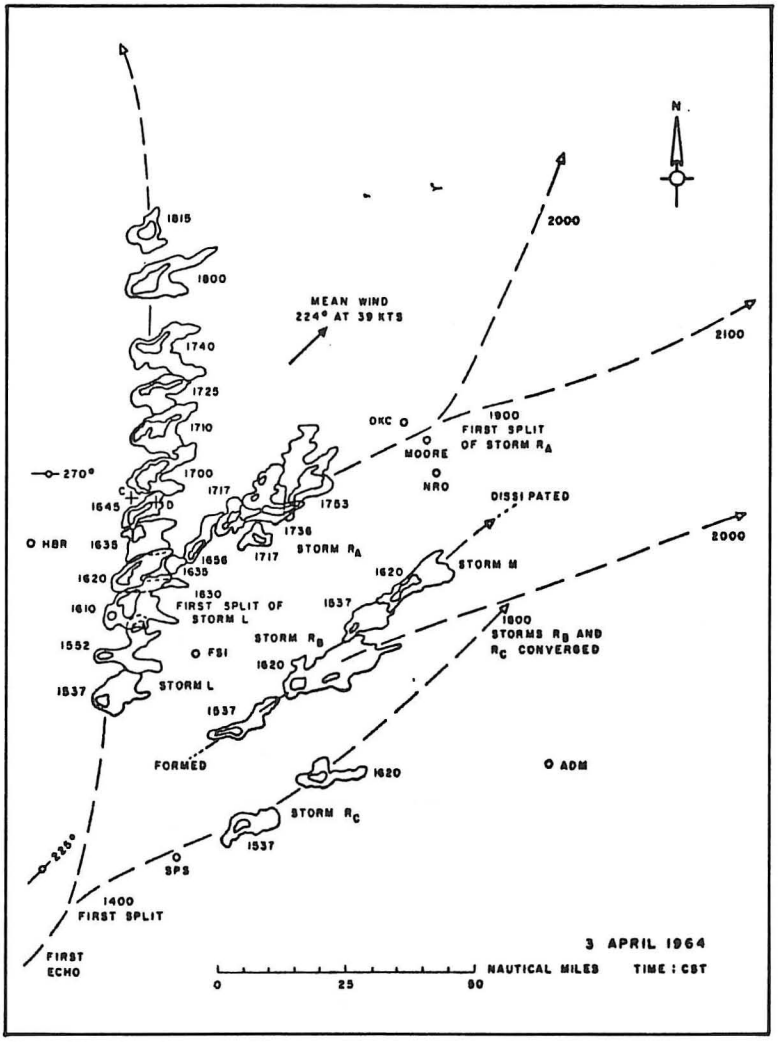

Fig. 9. Tracks of storm cells on 3 April 1964 (from Charba and Sasaki 1971) showing the persistence of both left- and right-moving cells.

which the shear is detrimental. There are solid theoretical reasons for the damping effect of shear on convection (see Newton 1963), but until recently (e.g., Rotunno and Klemp 1982) the enhancing effect of limited shear on convection was not well understood. It is now believed that the interaction of convection with the environmental wind shear can, under the right circumstances, favor continuing development of new convection (see Rotunno and Klemp 1982).

This brings up the issue of propagation, for which I can only give a too-brief discussion. It is important to understand that convective storms are not solid, unchanging things; they are the product of *processes*. The air parcels that make up a convective updraft change on a time scale of 20 min or so, and therefore the storm we "see" with our eyes or with radar is made up of a different set of parcels all the time. If interaction between the convective storm and the environmental wind creates new convection adjacent to the old convection sufficiently rapidly, we will "see" a storm which persists long after the original air parcels are long gone. I note that what we call storm *movement* is the sum of two contributions: *advection* and *propagation*. The convective storm is not simply a passive thing, carried along in the flow; rather, it is a process which can move by re-creating new convection on its own flanks.

Given a favorable range of shear, research (e.g., Klemp and Wilhelmson 1978, Weisman and Klemp 1984) has suggested that when the lowest several kilometers of the hodograph are curved, one member of the split pair (which develops in environments with straight hodographs) is favored over the other. This means that the favored one persists while the unfavored one dies out rapidly. It turns out that a *clockwise* turning of the hodograph favors the *cyclonic*, right-moving member of the split pair, while *counterclockwise* turning favors the *anticyclonic*, left-moving member (in the Northern Hemisphere, of course). The sort of storm most typical of a tornadic supercell is a cyclonically-rotating, right-moving storm; hence, this sort of storm becomes quite likely when the hodograph's lowest several kilometers are characterized by clockwise turning of the hodograph. However, this does not mean that supercells are limited to environments with clockwise-turning hodographs. The presence of substantial shear, even with straight-line hodographs, can be sufficient for supercells, under circumstances to be described below.

Consider the typical wind profile associated with mid-latitude storm systems: one finds a general increase of the wind's westerly component with height. This is a consequence of the fact that the temperature in the troposphere increases

equatorward, as one can verify using (1). In fact, this is a major part of the textbook explanation for the mid-latitude jet stream, which is quite intimately related to the severe thunderstorm environment.

How does one get a clockwise turning of the hodograph? First of all, there must be veering within the low levels of the atmosphere, but as shown in Figure 8, this by itself is not sufficient to produce clockwise turning of the hodograph. One ingredient that could be added to the wind profile in Figure 8 to yield an appropriate turning of the hodograph would be a low-level jet. Not only does that give the curve a clockwise turning (see Fig. 10), but it often serves to bring warm and moist air poleward at low levels, enhancing the convective instability (see Hess 1959, p. 100 ff.). Compare Figure 10 with Figure 11; although the details of Figure 10 are of no real significance, note that the primary change in the wind structure is within the layer from 1.5 to 3.6 km, with the winds generally backing and increasing in speed over the original values. For the actual case shown in Figure 11, the operational sounding at Oklahoma City at 1200 UTC did show a strong low-level jet, but this probably is a reflection of the nocturnal boundary layer wind maximum (see Blackadar 1957), so one might expect it to diminish in strength during the day. Instead, the later sounding shows that the winds in low levels backed and increased in speed, as illustrated schematically in Fig. 10. The afternoon sounding was released about 40 km east–southeast of an intense, tornadic supercell. On this particular day, a subsynoptic scale low pressure system was present to the west of the afternoon sounding site, which may have been responsible for the changes in the low-level flow, and the storm itself may have influenced the winds, of course.

Thus, all other things being equal (and they never are!), one may be able to use the hodograph to distinguish tornadic supercell days from those less likely to be tornadic. Pertinent questions of interest are: (1) How often does one get a sounding precisely at the time and place one needs it? (2) Is it valid to assume that the wind profile at 1200 UTC will remain unchanged right up to the point where storms begin to develop? (3) Without wind profilers and/or special sounding networks, is it impossible to anticipate changes in the hodograph?

Clearly, I believe the answers to these questions are: (1) Hardly ever. (2) No. (3) No. The reader is urged to look at Doswell and Maddox (1986) for some discussion of these topics in a more general framework, and at Korotky (1990) for a specific example. However, consider the following ideas. First of all, one can use changes in the surface data (primarily during the daytime) to diagnose and anticipate changes in the low-level wind profile. Backing and strengthening of the surface flow has long been recognized as a clue to the development of tornadic storms (see e.g., Tegtmeier 1974, Davies-Jones 1984). Such a change in the surface winds can be interpreted as a sign that a low-level jet is developing for dynamic reasons (e.g., strong pressure falls associated with the advancing and/or strengthening of a cyclone).

Thus, when one has reason to believe that a low-level cyclone is going to develop and/or move into the area, it is reasonable to expect an increase in the low-level flow.[5] It is possible to anticipate the development of a low-level jet in other ways available to an operational forecaster: the numerical model progs at the surface and 850 mb should show an increasing geostrophic wind, the forecast station data (the so-called "FOUS" output) should show backing and increasing surface winds, the winds aloft forecasts (the so-called "FD" winds) may even show such a low-level wind feature (although the models may not capture it well).

Hodographs change as the result of accelerations (positive or negative) throughout the troposphere. Thus, one can diagnose the flow upstream of the point in question at several levels and anticipate changes in the hodograph by the arrival of the upstream winds, yielding a crude forecast of the changes in the hodograph. If the current hodograph has little or no shear at the time of the sounding, but upstream shears are stronger, is it unreasonable to expect the hodograph to change? Certainly not, but one should not expect the upstream winds simply to be carried into the point in question without change. I make no bones about it: forecasting changes to the hodograph is not trivial, and it is unwise to assume that the hodograph will remain constant. Model predicted hodographs (Davies-Jones et al. 1990) can be helpful, but the model forecasts can be less than perfect.

The development of a middle-level minimum in a veering wind profile also can contribute to a clockwise turning of the lower part of the hodograph, but experience suggests that the middle level (say 700 to 500 mb) winds should not decrease to less than about 20 kt in the process if one is to maintain much severe storm potential. One way to have a middle-level minimum in the flow is to be just downstream of the axis of a difluent trough in middle levels. This latter situation has been associated frequently with substantial outbreaks of tornadic supercells. In classical situations, a negatively-tilted difluent trough in mid-levels also is coupled with a strong low-level jet (see Uccellini and Johnson 1979), yielding a wind profile such as shown in Fig. 11.

While I have said that it may be possible to anticipate the changes in the wind profile, it is not always the case that the changes take place on a scale large enough to be detected, much less anticipated. This means that what appears to be a case with lots of instability and not enough shear or a lack of hodograph turning can turn into something dramatically different on a very local scale. The result can be a brief, suprise tornado episode (see Burgess and Curran 1985, Burgess 1988); such developments are not uncommon, unfortunately. There are times when the clues are present but are sufficiently subtle that even a reasonably well-trained forecaster would have difficulty seeing those clues. It should be source of concern to every operational forecaster that even good people may not succeed in anticipating important events.

Moreover, not every storm developing in a large-scale environment with the "right" hodograph always will produce at least one tornado. Nor is it possible to say categorically that tornadoes only occur with the "right" kind of hodograph; there still is a lot we don't know about tornadoes and tornadic storms. Nevertheless, I dispute the notion that important severe weather events often arise "out of the blue," where there are no environmental clues that that day would be out of the ordinary. If one is not aware of the importance of the environmental wind structure, and is not well-trained in using hodographs to diagnose that structure and its evolution, it is understandable that one might fail to recognize a potentially dangerous situation.

It also appears (see Bluestein and Jain 1985) that squall

[5]If the cyclone is advancing at the same rate at every level in the troposphere, is it likely to be developing? I leave that for the reader to answer. If it *does* advance at the same rate throughout the troposphere, it will not increase the low-level flow in such a way as to create a low-level jet—rather, such a system would show increasing flow at all levels.

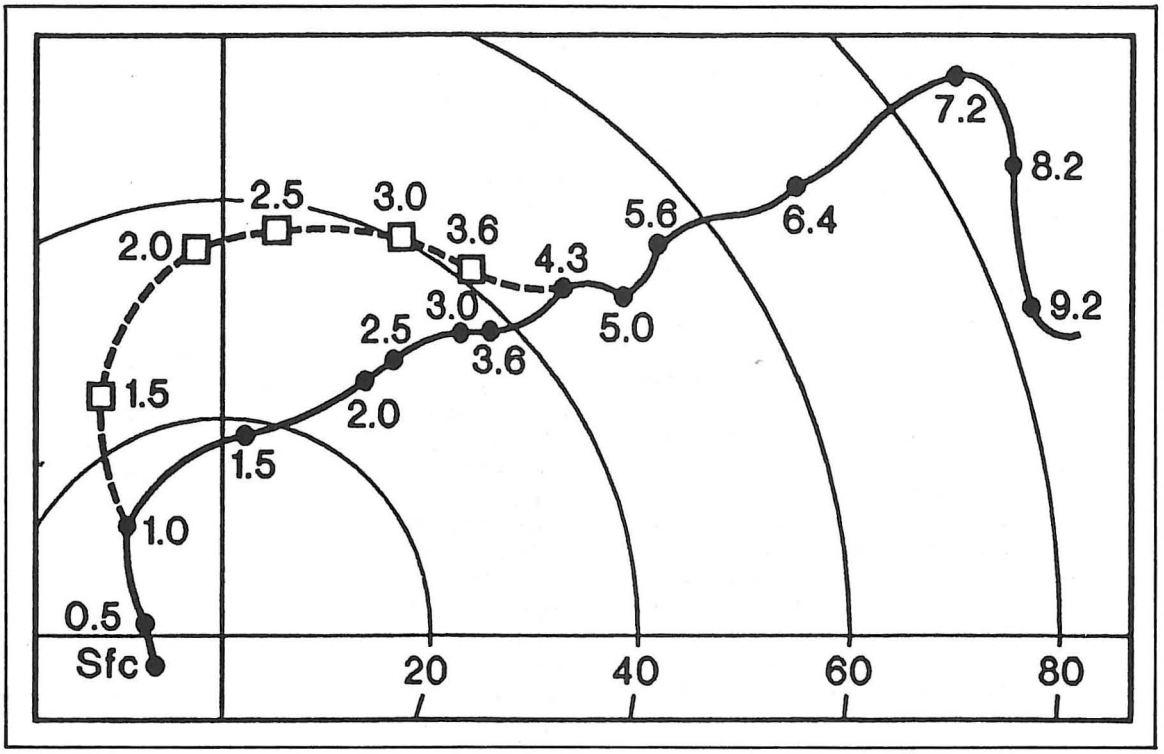

Fig. 10. Hypothetical changes (dashed line with open squares) to original 3 April 1964 hodograph (solid line with filled-in circles) that would result in substantial clockwise turning in the lowest 4 km. Wind speed circles, as in Fig. 8, are in kt.

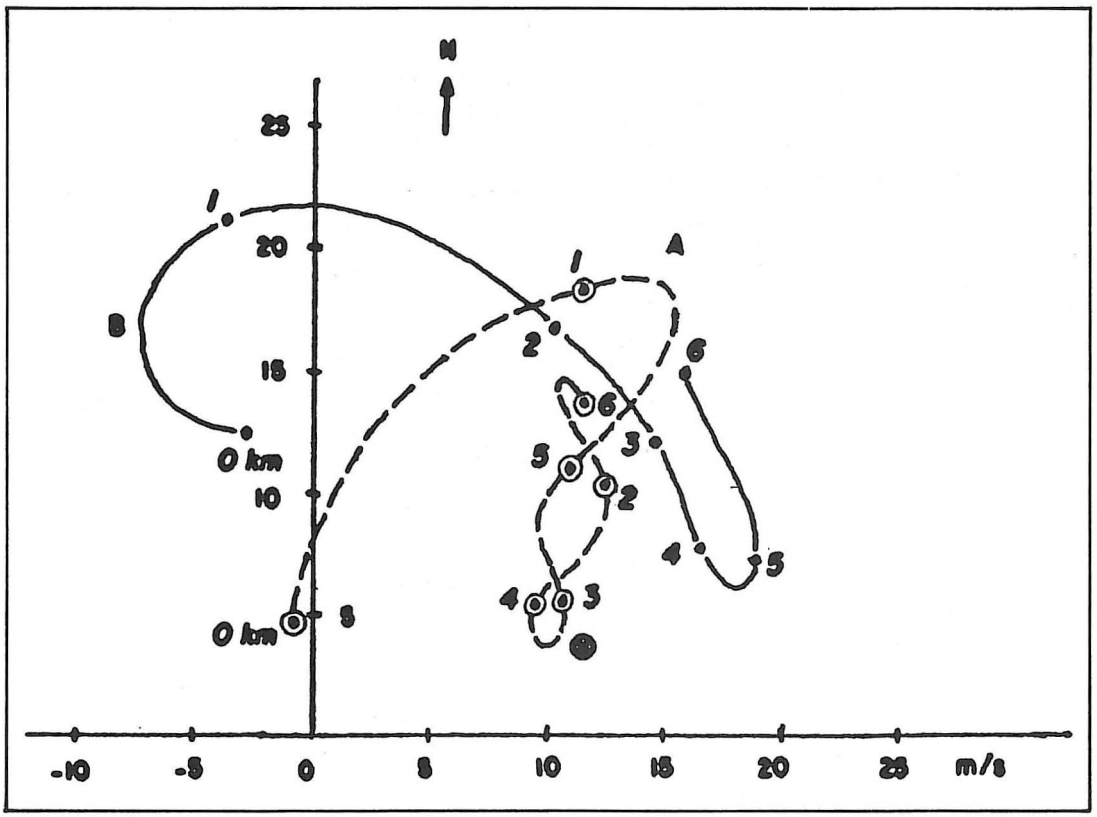

Fig. 11. Hodographs on 22 May 1981: (A) 1200 UTC at Oklahoma City, OK—and (B) 2015 UTC at Tuttle, OK with a violent tornado occurring near Binger, OK about 40 km away. Storm motion is indicated by the circled X.

line storms can occur in environments with hodographs that look rather like the supercell situation. If the environment seems to have a supercell-type shear structure, it is possible to observe either supercells or squall lines. Whenever the "right" sort of hodograph is present, the storm type may depend on the form of the low-level forcing: if it is localized, supercells are likely, whereas if it is along a line (e.g., a front), a squall line is the most probable outcome. I should emphasize that this interpretation is rather tentative at this point. Whatever differentiates between squall lines and supercells in these situations is as yet rather unclear. It remains possible, but still unproven, that differences in hodographs might control the atmosphere's choice (see Rotunno et al. 1988 and Fovell and Ogura 1989) between supercells and squall lines.

When the hodograph is not characteristic of supercells, other forms of convection are much more likely: multicell complexes and squall lines. Again, it seems that forcing along a line favors squall line development over complexes. Never forget that (a) subsynoptic structure can make the hodograph fit the supercell model locally and not be detected, and (b) the hodograph can change markedly from its morning appearance. Nevertheless, weak shear is characteristic of a lack of convective scale organization; individual storm cells are likely to have brief lifetimes and severe weather (if any) is sporadic, even though the convection as a whole may persist for relatively long times.

5. Vertical Wind Shear and Horizontal Vorticity

In striving to understand how the character of the hodograph influences convective storms, it is useful to digress somewhat and consider how vertical wind shear relates to vorticity. Most forecasters are probably familiar with vorticity maps, but they may not realize that vorticity is a *vector* quantity. Vorticity can be defined in several different, but equivalent ways; the most common way is that vector vorticity, denoted by $\boldsymbol{\omega}$, is the curl of the wind velocity vector ($\nabla \times \mathbf{V}$). The vector $\boldsymbol{\omega}$ can be broken down into its orthogonal Cartesian components, $\boldsymbol{\omega} = \xi\mathbf{i} + \eta\mathbf{j} + \zeta\mathbf{k}$, which also can be denoted by the ordered triplet of numbers (ξ, η, ζ), where

$$\xi \equiv \left(\frac{\partial w}{\partial y} - \frac{\partial v}{\partial z}\right), \eta \equiv \left(\frac{\partial u}{\partial z} - \frac{\partial w}{\partial x}\right), \zeta \equiv \left(\frac{\partial v}{\partial x} - \frac{\partial u}{\partial y}\right). \quad (2)$$

Many will recognize the third of these as the *relative vorticity* with which they are familiar. By adding the Coriolis parameter f to ζ, one obtains the *absolute* vorticity that one see plotted on conventional 500 mb "vorticity" maps. The quantity ζ is only the *vertical component* of the 3-dimensional vector vorticity, while there are two other, *horizontal* components.

The vorticity about a horizontal axis has been introduced in terms of the local orthogonal Cartesian coordinates. However, this is not the only way to look at it. In order to evaluate the horizontal part of the vorticity, it is a good approximation to ignore the contributions from the horizontal changes in vertical wind, so that the horizontal components of the vorticity in (2) can be approximated by

$$\xi \approx -\frac{\partial v}{\partial z}, \eta \approx +\frac{\partial u}{\partial z}. \quad (3)$$

This approximation can be shown to be equivalent to the hydrostatic approximation, which is pretty good in most situations not directly involving deep convection. Thus, the horizontal vorticity of the environment arises mostly from vertical changes in the horizontal wind—i.e., the vertical wind shear. If this approximation is made, it turns out that the horizontal vorticity vector is exactly perpendicular to the wind shear vector. This can be seen by breaking the total vorticity vector into two parts $\boldsymbol{\omega} = (\boldsymbol{\omega}_H, \zeta)$, where $\boldsymbol{\omega}_H$ is the horizontal vorticity vector ($\boldsymbol{\omega}_H = \xi\mathbf{i} + \eta\mathbf{j}$), and ζ is the (scalar) vertical component. It is easy to show from vector identities that (3) can be summarized as:

$$\boldsymbol{\omega}_H = \mathbf{k} \times \frac{\partial \mathbf{V}_H}{\partial z}, \quad (4)$$

where $\mathbf{k}$ is the unit vector in the vertical. Now (4) says that the resulting horizontal vector vorticity is 90° to the left (as one looks down the hodograph in the direction of increasing height) of the shear vector, by using the right-hand rule for evaluating the direction of the vector resulting from the cross product.

All one really needs to know is that for the large-scale environment (when the contribution from vertical motion is negligible), the horizontal vorticity vector can be treated as being exactly 90° to the left of the shear vector (see Fig. 12). Using this, one might imagine horizontal vorticity vectors all along the hodograph. A simple way to visualize this horizontal vorticity is to imagine one is looking at *unidirectional* sheared flow (Fig. 13).[6] The shear clearly is acting to rotate a solid object in the flow as shown in the figure; a useful mental image is a kicked football rotating end over end. Unfortunately, this simple picture can be misleading in two ways. First, the inferred sense of rotation does not imply the actual existence of upward motion on the left and downward motion on the right (in the figure). Rather, the fluid (the atmosphere is a fluid, of course) at one level is sliding horizontally past the fluid at levels above and below. While it is possible that such vertical circulations exist, they are not always present in vertically sheared flows.

Second, this simple picture is not appropriate whenever wind direction, as well as speed, changes with height. In thinking about the situation when only wind speed changes

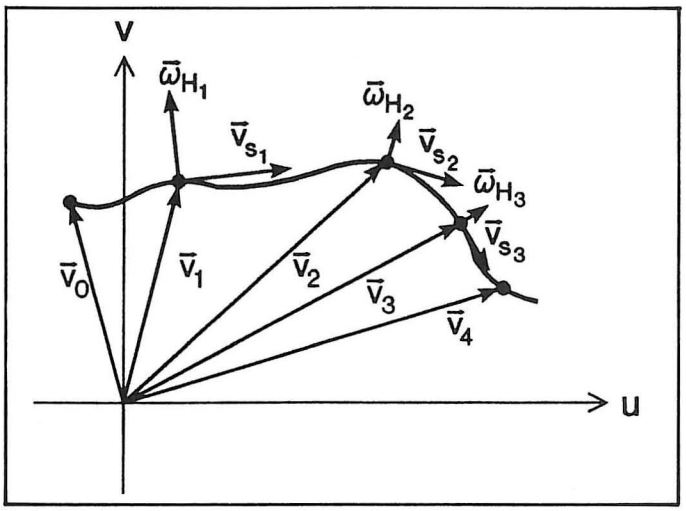

Fig. 12. Hodograph showing the horizontal vorticity vectors associated with selected shear vectors.

[6]Note that in the case of unidirectional flow with shear, the flow is equivalent barotropic (recall the discussion in Sec. 3a).

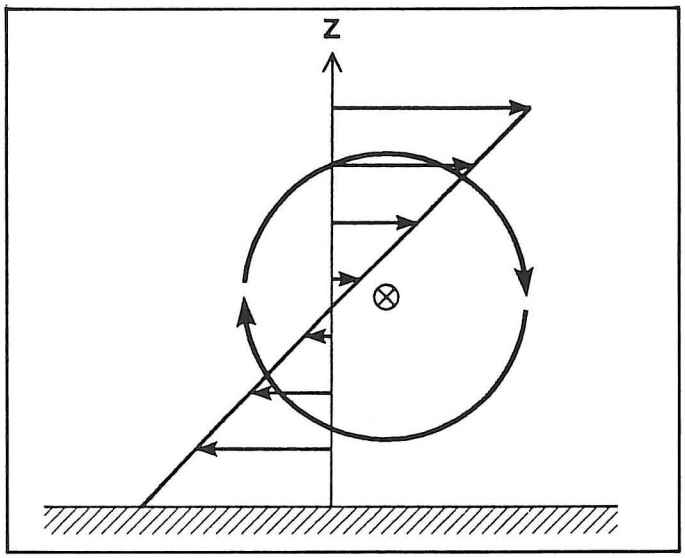

Fig. 13. Schematic illustration of how horizontal vorticity is associated with shear in unidirectional flow, with the circled "X" indicating the vorticity vector pointing into the page.

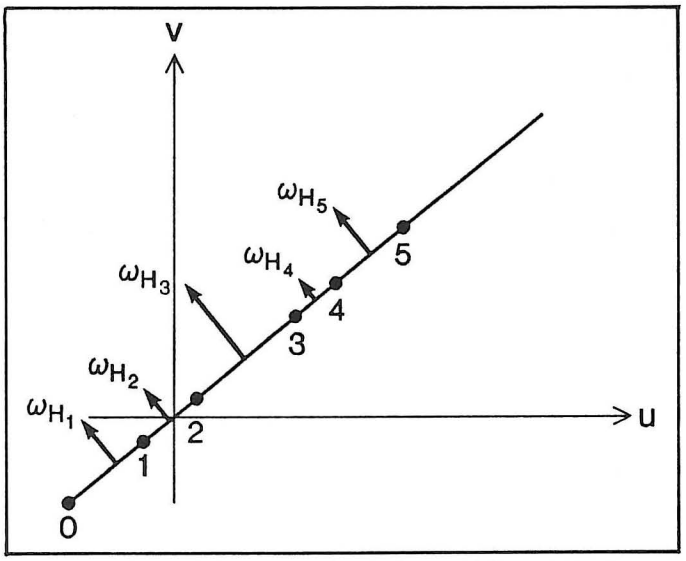

Fig. 14. Hodograph for undirectional flow, which must lie along a radial—i.e., its extension must pass through the origin. Indicated on the hodograph are the winds at, say, 0 to 5 km, and the horizontal vorticity vectors associated with the layer 0–1 km, 1–2 km, etc.

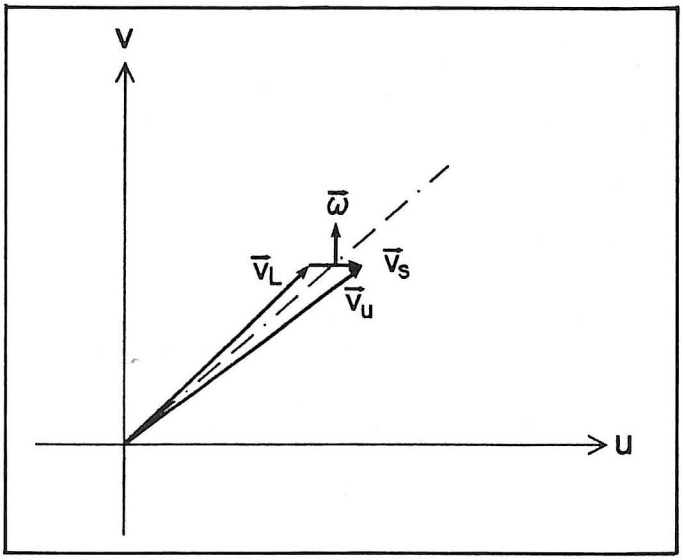

Fig. 15. Illustration of the calculation of the shear and the associated horizontal vorticity for a thin layer.

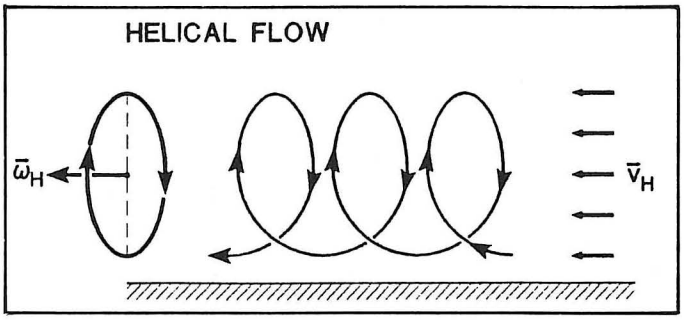

Fig. 16. Schematic showing how the superposition of horizontal vorticity (ω_H) parallel to the horizontal flow (V_H) produces a helical flow.

with height, it can be seen (Fig. 14), that the horizontal vorticity vector is perpendicular to the flow at all levels. Note that the shear vectors are not shown in Figure 14 because they plot directly over the hodograph. When the wind direction changes with height, it becomes possible for some component of the horizontal vorticity vector to be aligned parallel (or antiparallel) to the flow.

In order to see the general case, consider a very shallow layer over which the shear is measured, as in Figure 15. Although the layer used in Figure 15 is of finite depth, note that the mean wind in that layer is very similar to the wind at either the top or the bottom. In this example, both wind speed and wind direction are changing; in the limit as the depth of the layer shrinks to zero, the finite shear vector becomes the vertical derivative of the horizontal wind. It can be seen that one part of the horizontal vorticity is parallel to the flow in that layer and another is perpendicular. This way of looking at $\boldsymbol{\omega}_H$ leads to the terminology of *streamwise* vorticity (that which is *parallel* to the wind) and *crosswise* vorticity (that which is *perpendicular* to the wind). Such a viewpoint turns out to be more meaningful physically than the orthogonal Cartesian components (ξ, η) of $\boldsymbol{\omega}_H$ (see Davies-Jones 1984). That is, the horizontal vorticity can be decomposed as $\boldsymbol{\omega}_H = \omega_s \mathbf{e}_s + \omega_c \mathbf{e}_c = (\omega_s, \omega_c)$, where $\mathbf{e}_s$ and $\mathbf{e}_c$ are unit vectors in the streamwise and crosswise directions, respectively (i.e. they are parallel and perpendicular to the flow),[7] while ω_s and ω_c are the streamwise and crosswise components of vorticity.

In the case of streamwise vorticity, which is present only when the wind direction changes with height (again, neglecting the contribution from vertical motion's horizontal gradient), one can visualize the flow as being helical (Fig. 16); a good mental image is a passed football rotating in a "spiral." Hence, the term *helicity* is associated directly with streamwise vorticity. As with Figure 13, however, one should not

[7]These unit vectors can also be thought of as those associated with the so-called *natural* coordinate system (see e.g., Hess 1959, pp. 177 ff.)

interpret Figure 16 to show actual parcel trajectories. Again, the flow can be purely horizontal, with air at one level simply sliding past that at levels above and below. The vertical motions need not be present, but this picture does give a correct sense of the horizontal vorticity vector (using the right-hand rule, of course) associated with this sheared flow.

It is the relationship between the horizontal vorticity vector ($\boldsymbol{\omega}_H$) and the horizontal velocity vector ($\mathbf{V}_H$) that allows a precise definition of helicity. Note that $\mathbf{V}_H = V\mathbf{e}_s$, so that $\mathbf{V}_H \cdot \boldsymbol{\omega}_H = V\omega_s \equiv h$, where h is the *local* value of helicity; it is a local value in the sense that $\mathbf{V}_H$ and $\boldsymbol{\omega}_H$ can vary from point to point in the field, including from one level to another in the sounding. Since this local value may not be representative of the sounding as a whole, it is common to determine a vertically-integrated value (similar to a vertical average) over some layer in hopes of finding a meaningful number. This vertically-integrated helicity (H) is defined as:

$$H \equiv \int_{z_0}^{z_1} \mathbf{V}_H \cdot \boldsymbol{\omega}_H \, dz, \qquad (5)$$

where in this case, this is the integrated helicity over the layer from z_0 to z_1. Terminology may well vary, and both H and h may be referred to as "helicity" in the various reference sources. It is important to be sure which is being referred to when reading these sources.

6. The Importance of Storm-Relative Flow

In the preceding discussion, all the concepts were developed in a ground-relative framework. However, the notion that we must make some changes for moving coordinate systems has already been mentioned. Consider the effect of storm motion on the flow as seen by an observer moving along with the storm. Given a particular wind vector **V** as shown in Figure 17, for a storm moving with a vector velocity **C**, the wind in a storm-relative framework can be obtained by subtracting out the storm motion; i.e., we define the relative flow $\mathbf{V}_r$ to be $\mathbf{V} - \mathbf{C}$. Thus, for a hodograph as given in Figure 18, the storm-relative wind vectors are as shown. Observe that while the vectors have changed, the *hodograph* has remained unchanged. When one does a transformation using a constant velocity (in this case, **C**), it is known as a

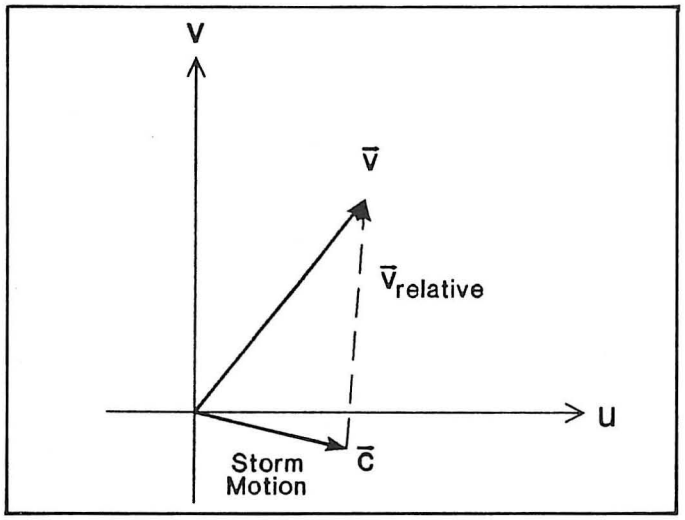

Fig. 17. Example of how one obtains the storm relative wind $\mathbf{V}_r$ by subtracting the storm motion **C** from the ground-relative wind **V**.

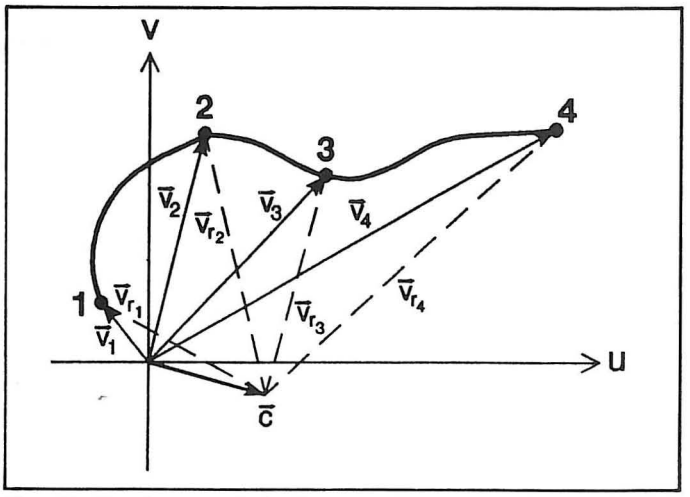

Fig. 18. For the sample hodograph shown, several wind vectors are shown in both ground-relative (solid arrows) and storm-relative (dashed arrows) frameworks, where **C** denotes storm motion.

Galilean transformation. Since the hodograph remains unchanged during a Galilean transformation, it is said to be *Galilean invariant*. If, as is common, the storm motion is not constant (in both speed and direction, of course), the problem becomes much more complicated. I shall not consider accelerated coordinate frames here, so the following discussion only applied to situations where C remains constant.

When the flow changes direction with height, the simplest possible case is for the shear to be unidirectional; i.e., the hodograph is still a straight line (Fig. 19). In such a case, however, the vorticity vector is no longer strictly perpendicular to the flow at all levels; in fact, there may be considerable streamwise vorticity (or helicity) in such a situation. If the storm moves such that its motion vector is anywhere *along* the line containing the hodograph, what does the flow look like in a storm-relative framework? Hopefully, it is easy to see that by subtracting out the storm motion vector in such a

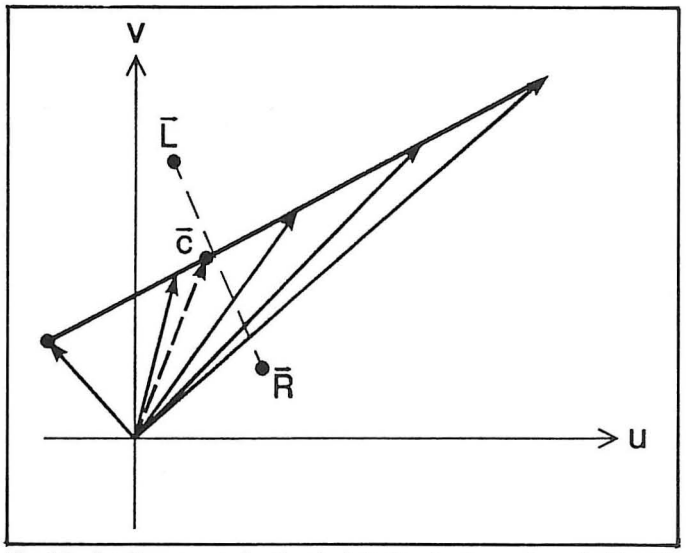

Fig. 19. Another example of a straight-line hodograph, as in Fig. 14, but in this case the flow is not unidirectional, so the hodograph does not lie along a radial passing through the origin. Vectors **L** and **R** denote storm motions for left- and right-moving storms, respectively.

situation, all the flow ends up being parallel to the hodograph. Therefore, in the case of a straight line hodograph and a storm moving with a velocity somewhere along the straight line containing the hodograph, an observer traveling with the storm does not "see" any streamwise vorticity, even if there is some present in a ground-relative sense. For such a storm to encounter streamwise vorticity in a storm-relative sense, its motion must be somewhere *off* the hodograph. Figure 19 shows a typical splitting storm situation, which shows the left- and right-movers having storm motions off the hodograph and so an observer travelling with such storms "sees" storm-relative streamwise vorticity. Note that in the formula just presented in the previous section for helicity, one obtains the *storm-relative* helicity by replacing $\mathbf{V}_H$ with $\mathbf{V}_H - \mathbf{C}$ (see Davies-Jones et al. 1990).

Streamwise vorticity (or helicity) clearly is *not* independent of the motion of the coordinate frame. If such a quantity is not Galilean invariant, it seems logical that the only coordinate framework that is physically meaningful is one fixed to the storm itself—it is within this framework that the storm "sees" its environment.

When the hodograph is curved, the storm motion is much more likely to lie somewhere off the hodograph. In this case, it can be shown that the simple average of the winds lies somewhere "inside" the curve of the hodograph. Since the advective part of the storm motion usually is considered to arise from the vertically-averaged winds in the storm-bearing layer, such a component of storm motion normally lies off the hodograph when it is curved.

Even if storm motion does happen to lie on the hodograph in the curved hodograph case, it should be clear that streamwise vorticity can still exist at levels above and below that point on the hodograph corresponding to storm motion. For curved hodographs, then, it is likely that storms will encounter considerable storm-relative helicity.

In either a ground-relative or a storm-relative case, a flow which only changes direction with no change in speed (i.e., a hodograph which is a segment of a circle centered on the origin) has *only* streamwise vorticity. As shown in Davies-Jones et al. (1990), the vertically-integrated helicity is proportional (by a factor of -2) to the area swept out by the wind vectors along the hodograph (Fig. 20). This means that the storm motion can increase or decrease the storm-relative helicity associated with a given hodograph, including change its sign. Thus, there are storm motions that can make the storm-relative helicity (averaged over some fixed layer) vanish; one example (there are infinitely many of them) is shown in Figure 21. Storm motions can lie anywhere on the hodograph, and it is possible to draw contours of storm-relative helicity (see Fig. 1 in Davies-Jones et al. 1990). If one were to change the layer over which the local helicity is integrated in such a situation, the integrated helicity contours would be different, of course.

Many researchers now believe it is the *storm-relative* helicity in the lowest two or three kilometers of the atmosphere which is most relevant to the likelihood of supercell behavior with storms in that environment. This layer is, crudely, the one over which most of the storm's inflow occurs, so there is at least some reason to accept this on physical terms. Davies-Jones et al. (1990) suggest that for the 0–3 km layer, one can associate weak, strong, and violent mesocyclones with storm-relative integrated helicity values of 150–299, 300–449, and ≥ 450 m^2 s^{-2}, respectively. However, one should not take these as hard and fast rules. As noted in Davies-Jones et al. (1990), test results using these thresholds are encouraging, but not perfect. Some of the forecast problems using these thresholds may well lie in the fact that inflow layer depths are not always the same from situation to situation.

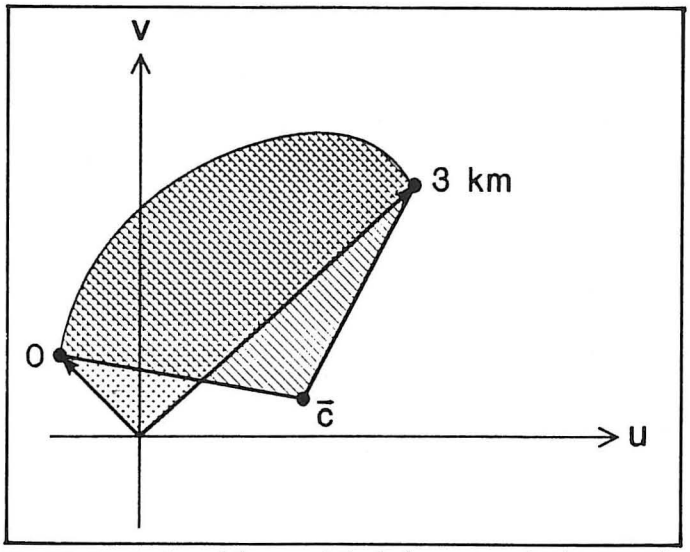

Fig. 20. Illustration of the area (stippled) swept out by the ground-relative wind vectors along the hodograph from 0 to 3 km. Also shown is the area swept out by the storm-relative wind vectors (hatched).

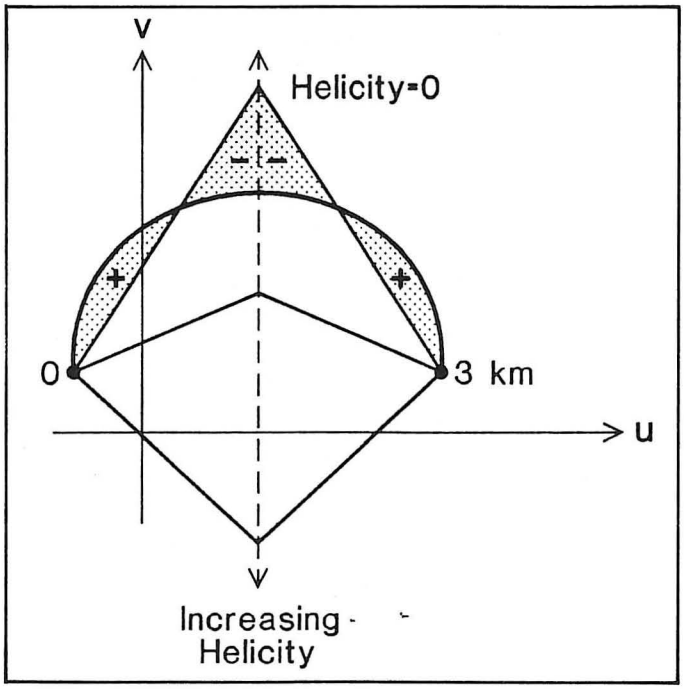

Fig. 21. An example of the changes in storm-relative helicity, integrated over the layer from 0 to 3 km, as a function of the storm motion (**C**). In this example, changes in **C** are limited to changes in the north–south component, so **C** moves only upward or downward along the dashed line. There is a point (indicated) where the negative and positive areas cancel and the resulting total storm-relative helicity averaged over the layer vanishes.

7. Final Remarks

Although the relationship of a storm's structure and behavior to its environment is not yet completely understood, it is clear that our ability to forecast the probable evolution of convective storms depends on that relationship. Years of observations and research have suggested that this is not an entirely fruitless avenue to pursue. As with any diagnostic tool, hodograph analysis does not provide the user with black-and-white "answers" to forecast problems.

With time, it has become increasingly apparent that supercell storms are physically distinct from other forms of convection. Moreover, it appears that supercellular behavior is intimately related to the character of the environmental hodograph. As suggested in Davies-Jones et al. (1990), there may be ways to predict storm structure based on parameters derived from hodographs. However, it is unlikely that there are "magic" thresholds that reliably distinguish between events. As with thermodynamic indices derived from the temperature-hmidity part of a sounding, indices based on the hodograph provide only some of the information contained in the hodograph itself. Therefore, it seems prudent for forecasters to develop (or refresh) their ability to interpret and use hodographs.

Since storm motion is so critical to the presence or absence of storm-relative helicity, our ability to forecast storm motion has become an important link in forecasting behavior of convective storms. This topic, unfortunately, is beyond the scope of this paper; further, it is not yet clear that any comprehensive methodology for anticipating storm motion is available (see, however, Colquhoun and Shepherd 1989). Part of the problem with forecasting movement of convective storms is that some aspects of storm motion are governed by processes internal to the storm itself, whereas external processes (those that exist independent of the convection) may be quite important in some situations (see Doswell et al. 1990).

This somewhat unsatisfactory situation can be interpreted optimistically, however. A forecaster attempting to apply the hodograph to forecasting the occurrence of supercell convection must attempt to foresee the limits on the possible forms the hodograph can assume. That is, the forecaster must determine whether or not a hodograph favorable to supercells is possible, in his or her best meteorological judgement. If it is to be possible, then I have shown that one must account for the storm motion; given a plausible forecast of the hodograph, what sorts of storm motions will enhance the chances for supercells? If the forecaster's awareness of the supercell potential is heightened, then when storms develop and move in ways that are consistent with this analysis, the forecaster is prepared to look at them carefully for supercell characteristics. In other words, the chance of detecting and recognizing supercells is enhanced substantially if one has anticipated their potential occurrence long before they develop. I have tried to indicate the importance of using hodographs for this task.

While this brief paper has provided some broad overview of hodographs, I cannot overemphasize the importance of reading the references. There is no way I can offer much more than an introduction to a topic which touches on many areas and which contains many subtleties. I especially recommend that the reader review the three papers by Weisman and Klemp (1982, 1984, 1987), as well as Davies-Jones et al. (1990) and the review by Klemp (1987).

Finally, it has come to my attention recently that a PC-based interactive sounding analysis package, called SHARP (for Skew-T/Hodograph Analysis and Research Program), has been developed for use in operational forecasting offices. I encourage interested readers to pursue its use in forecasting, especially with regard to its analysis of hodographs.

Acknowledgments

I am particularly grateful to Dr. Robert Davies-Jones, who has been patient with my efforts to understand the subtleties of hodograph interpretations and willing to correct my errors with a firm hand. Dr. Harold Brooks, Mr. Rod Gonski and the anonymous reviewers made many helpful suggestions to improve the paper. Also, Ms. Joan Kimpel improved my original crude figures by a large margin and her assistance is greatly appreciated. The substance of this paper appeared earlier in an informal publication by NWS Southern Region Headquarters, thanks to Dan Smith and Lans Rothfusz of Southern Region's Scientific Services Division.

Author

Charles A. Doswell III received his B.S. in Meteorology at the University of Wisconsin in 1967, his M.S. in Meteorology at the University of Oklahoma in 1969, and after serving with the Army in Vietnam and at White Sands Missile Range, New Mexico, received his Ph.D. in Meteorology at the University of Oklahoma in 1976. In addition to his present employment with the National Severe Storms Laboratory in Norman, Oklahoma, he has worked at the National Severe Storms Forecast Center in Kansas City, Missouri, and the Environmental Research Laboratories in Boulder, Colorado. His research interests include all aspects of weather forecasting (including verification), objective analysis, and virtually everything connected to severe storms (from cloud physics to the general circulation).

References

Blackadar, A. K., 1957: Boundary layer wind maxima and their significance for the growth of nocturnal inversions. *Bull. Amer. Meteor. Soc.*, 5, 283–290.

Bluestein, H. B., and M. H. Jain, 1985: Formation of mesoscale lines of precipitation: Severe squall lines in Oklahoma during the spring. *J. Atmos. Sci.*, 42, 1711–1732.

Braun, S. A., and J. P. Monteverdi, 1991: An analysis of a mesocyclone-induced tornado occurrence in northern California. *Wea. Forecasting*, 6, 13–31.

Burgess, D. W., 1988: The environment of the Edmond, Oklahoma tornadic storm. *Preprints, 15th Conf. Severe Local Storms* (Baltimore, MD), Amer. Meteor. Soc., 293–294.

Burgess, D. W. and E. B. Curran, 1985: The relationship of storm type to environment in Oklahoma on 26 April 1984. *Preprints, 14th Conf. Severe Local Storms* (Indianapolis, IN), Amer. Meteor. Soc., 208–211.

Charba, J., and Y. Sasaki, 1971: Structure and movement of the severe thunderstorms of 3 April 1964 as revealed from radar and surface mesonetwork data analysis. *J. Meteor. Soc. Japan*, 49, 191–213.

Colquhoun, J. R., and D. J. Shepherd, 1989: An objective basis for forecasting tornado intensity. *Wea. Forecasting*, 4, 35–50.

Davies-Jones, R. P., 1984: Streamwise vorticity: The origin of updraft rotation in supercell storms. *J. Atmos. Sci.*, 41, 2991–3006.

Davies-Jones, R., D. W. Burgess, and M. Foster, 1990: Test of helicity as a tornado forecast parameter. *Preprints, 16th Conf. Severe Local Storms* (Kananaskis Park, Alberta), Amer. Meteor. Soc., 588–592.

Doswell, C. A. III, 1982: The Operational Meteorology of Convective Weather. Vol. I: Operational Mesoanalysis. *NOAA Tech. Memo. NWS NSSFC-5,* Available from author at National Severe Storms Lab, 1313 Halley Circle, Norman, OK 73069, pp. II-2–II-14 and II-28–II-31.

Doswell, C. A. III, and R. A. Maddox, 1986: The role of diagnosis in weather forecasting. *Preprints, 11th Conf. Wea. Forecasting and Analysis* (Kansas City, MO), Amer. Meteor. Soc., Boston, 177–182.

Doswell, C. A. III, A. R. Moller, and R. Przybylinski, 1990: A unified set of conceptual models for variations on the supercell theme. *Preprints, 16th Conf. Severe Local Storms* (Kananaskis Park, Alberta), Amer. Meteor. Soc., 40–45.

Fovell, R. G., and Y. Ogura, 1989: Effect of vertical wind shear on numerically simulated multicell storm structure. *J. Atmos. Sci.*, 46, 3144–3176.

Gonski, R. F., B. P. Woods, and W. D. Korotky, 1989: The Raleigh tornado—20 November 1988. An operational perspective. *Preprints, 12th Conf. Wea. Analysis and Forecasting* (Monterey, CA), Amer. Meteor. Soc., 173–178.

Hess, S. L., 1959: *Introduction to Theoretical Meteorology.* Holt, Rinehart and Winston, New York, p. 276 ff.

Holton, J. R., 1979: The planetary boundary layer. *An Introduction to Dynamic Meteorology* (2nd ed.), Academic Press, New York, 106–113.

Klemp, J. B., 1987: Dynamics of tornadic thunderstorms. *Ann. Rev. Fluid Mech.*, 19, 369–402.

Klemp, J. B., and R. B. Wilhelmson, 1978: Simulations of right- and left-moving storms produced through storm splitting. *J. Atmos. Sci.*, 35, 1097–1110.

Korotky, W. D., 1990: The Raleigh tornado of November 28, 1988: The evolution of a tornadic environment. *Preprints, 16th Conf. Severe Local Storms* (Kananaskis Park, Alberta), Amer. Meteor. Soc., 532–537.

Newton, C. W., 1963: Dynamics of severe convective storms. *Meteor. Monogr.*, 5, No. 27 (D. Atlas, Ed.), Amer. Meteor. Soc., Boston, Mass., 33–58.

Oliver, V. J., and M. B. Oliver, 1945: Weather analysis from single-station data. *Handbook of Meteorology* (F. A. Berry, E. Bollay, and N. R. Beers, eds.), McGraw-Hill, New York, 858–879.

Rasmussen, E. N., and R. B. Wilhelmson, 1983: Relationships between storm characteristics and 1200 GMT hodographs, low-level shear, and stability. *Preprints, 13th Conf. Severe Local Storms* (Tulsa, OK), Amer. Meteor. Soc., J5–J8.

Rotunno, R., and J. B. Klemp, 1982: The influence of the shear-induced vertical pressure gradient on thunderstorm motion. *Mon. Wea. Rev.*, 110, 136–151.

Rotunno, R., J. B. Klemp, and M. L. Weisman, 1988: A theory for strong, long-lived squall lines. *J. Atmos. Sci.*, 45, 463–485.

Schaefer, J. T. and C. A. Doswell III, 1980: The theory and practical application of antitriptic balance. *Mon. Wea. Rev.*, 108, 746–756.

Stone, H. M., 1988: Convection Parameters and Hodograph Program—CONVECTA and CONVECTB. *NOAA Tech. Memo. NWS ERCP No. 37 (revised),* Scientific Services Division, Bohemia, NY 11716, 44 pp.

Tegtmeier, S. A., 1974: The role of the surface, sub-synoptic low pressure system in severe weather forecasting. M. S. Thesis, Univ. of Oklahoma, Dep't of Meteorology, Norman, OK, 66 pp.

Uccellini, L. W., and D. R. Johnson, 1979: The coupling of upper and lower tropospheric jet streaks and implications for the development of severe convective storms. *Mon. Wea. Rev.*, 107, 682–703.

Weisman, M. L., and J. B. Klemp, 1982: The dependence of numerically simulated convective storms on vertical wind shear and buoyancy. *Mon. Wea. Rev.*, 110, 504–520.

Weisman, M. L., and J. B. Klemp, 1984: The structure and classification of numerically simulated convective storms in directionally varying wind shears. *Mon. Wea. Rev.*, 112, 2479–2498.

Weisman, M. R., and J. B. Klemp, 1987: Characteristics of isolated convective storms. *Mesoscale Meteorology and Forecasting* (P. S. Ray, ed.), Amer. Meteor. Soc, Boston, 341–358.